An Unbiased Groupwise Registration Algorithm for Correcting Motion in Dynamic Contrast-Enhanced Magnetic Resonance Images

Mia Mojica and Mehran Ebrahimi(✉)

Faculty of Science, University of Ontario Institute of Technology,
2000 Simcoe Street North, Oshawa, ON L1H 7K4, Canada
{mia.mojica,mehran.ebrahimi}@uoit.ca
http://www.ImagingLab.ca/

Abstract. A simple and computationally efficient algorithm for performing unbiased groupwise registration to correct motion in a dataset of contrast-enhanced magnetic resonance (DCE-MR) images is presented. All the DCE-MR images in the sequence are registered simultaneously and updates to the reference are computed using an averaging technique that takes into account all the transformations aligning each image to the current reference. The method is validated both subjectively and quantitatively using an abdominal DCE-MRI dataset. When combined with the normalized gradient field dissimilarity measure, it produced promising results and showed significant improvements compared to those obtained from an existing motion correction approach.

Keywords: DCE-MRI registration · Multilevel elastic registration
Normalized gradient field · Groupwise registration

1 Introduction

Over the last years, dynamic contrast-enhanced magnetic resonance imaging (DCE-MRI) has been a useful clinical technique in the characterization of tumor biology. It involves the acquisition of a sequence of images acquired pre- and post-injection of a bolus of a contrast agent. The uptake of the contrast agent from this sequence of images can be quantified via a concentration vs. time curve, which in turn allows us to characterize vascular permeability [13].

DCE-MRI continues to be a crucial component in identifying appropriate patient treatment response. However, motion present in the dataset has to first be compensated to accurately convert signal intensity changes to contrast agent concentrations [7]. Image registration has been demonstrated to be effective in obtaining a motionless dataset from a sequence of DCE-MR images [1,2,6,8].

Some registration methods for DCE images include reducing motion in the dataset through a floating image reference scheme combined with principal component analysis, as presented in [7]. In their paper, an intensity correction term

D. Stoyanov et al. (Eds.): RAMBO 2018/BIA 2018/TIA 2018, LNCS 11040, pp. 42–52, 2018.
https://doi.org/10.1007/978-3-030-00946-5_5

was added to the similarity measure for pairwise registration. In [12], the registration problem was divided into sub-problems using auxiliary images computed from the conditional probability distribution of image pairs. These auxiliary images were registered to the original images using the sum of squared differences.

We introduce a groupwise registration approach combined with an NGF-based pairwise step for correcting motion and subsequently validate the proposed scheme on a set of abdominal dynamic contrast-enhanced MR images. The groupwise framework used in this paper assumes equal weight for all pairwise transformations to come up with an update to the reference image. It effectively reduces naturally occurring motion induced by the respiration process and is able to align images in spite of the changes in contrast.

2 Pairwise Registration

Constructing a motion-corrected dataset through groupwise registration entails aligning the subjects to the same reference geometry. In this paper, we used a combination of affine and elastic (also referred to as "non-parametric registration"in [9]) to initialize each groupwise iteration.

2.1 Mathematical Model

Given a template and a reference image $\mathcal{T}, \mathcal{R} : \Omega \subset \mathbb{R}^2 \to \mathbb{R}$, we wish to find a transformation $y : \Omega \to \mathbb{R}^2$ such that a transformed version $\mathcal{T}[y]$ of the template image $\mathcal{T}$ is similar to the reference $\mathcal{R}$. This is equivalent to the optimization problem

$$\min_y \mathcal{J}[y] = \mathcal{D}[\mathcal{T}[y], \mathcal{R}] + \alpha \mathcal{S}[y]. \tag{1}$$

The term $\mathcal{D}$ in the joint functional $\mathcal{J}$ is called a distance measure and it quantifies the similarity between the transformed template and the reference image. The second term $\mathcal{S}$ is the regularization term, which makes the registration problem well-posed.

In our implementations, we have tested the following distance measures:

a. Normalized Gradient Field (NGF)

$$\mathcal{D}^{\mathrm{NGF}}[\mathcal{T}, \mathcal{R}] = \mathrm{NGF}[\mathcal{T}, \mathcal{R}] = \int_\Omega 1 - \left(\mathrm{NGF}[\mathcal{T}(x)]^T \mathrm{NGF}[\mathcal{R}(x)]\right)^2 dx \tag{2}$$

where $\mathrm{NGF}[\mathcal{T}]$ denotes the normalized gradient field of $\mathcal{T}$, defined by

$$\mathrm{NGF}[\mathcal{T}] = \mathrm{NGF}[\mathcal{T}, \eta] = \frac{\nabla \mathcal{T}}{\sqrt{|\nabla \mathcal{T}|^2 + \eta^2}}$$

and η is an edge parameter. The NGF is suited for aligning images where intensity changes appear at corresponding positions. These intensity changes are given by the image gradient $\nabla \mathcal{T}$.

b. Sum of Squared Differences with Intensity Correction (SSDIC)
In [7], intensity correction was used in combination with the SSD to partially account for intensity changes between image volumes. Instead of solving for a reasonable transformation aligning $\mathcal{T}$ and $\mathcal{R}$, we find one that matches the "intensity-corrected" template T^c to the reference, where

$$\mathcal{T}^c = \mathcal{T} + c, \quad c = (\mathcal{R} - \mathcal{T}) * \mathrm{N}(0, \sigma),$$

and $\mathrm{N}(0, \sigma)$ is a Gaussian kernel with a mean and standard deviation of 0 and σ, respectively. The template image is transformed using the optimal deformation aligning the intensity-corrected template to the reference image.

The above distance measures are approximated using a midpoint quadrature rule on a cell-centered grid with uniform mesh spacing.

2.2 Multilevel Affine and Elastic Registration

The discretized form of the registration problem in (1) is solved from the coarsest to the finest level. We perform an affine registration at the coarsest level and use the resulting optimal transformation to initialize y^{ref} in the regularization term $\mathcal{S}[y]$, which is given by the elastic potential of the transformation y [9]:

$$\mathcal{S}[y] = \text{Elastic Potential}\left[y - y^{\mathrm{ref}}\right].$$

The starting guess for the optimal transformation at every succeeding level is taken to be the prolongated version of the solution y^h from the preceding level.

3 Groupwise Registration

Groupwise registration has been used in a wide range of applications, including normalizing structural and functional MR data [3]. In [5], the performance of a groupwise registration method with a principal component analysis-based metric for correcting motion in DCE-MR images of the liver was evaluated.

Here, we adopt the method used in [4,11] to correct motion in a sequence of DCE-MR images and coupled it with the pairwise registration step discussed in the previous section.

Each groupwise iteration is initialized by mapping every image in the dataset to the current reference image. The reference image is then updated using an averaging technique that takes into account all the transformations obtained from the pairwise registration step. The update to the reference is given by

$$\mathcal{R}^{n+1}_{\mathrm{mean}}(\mathrm{x}^h) = \frac{1}{N}\sum_{i=1}^{N} \mathcal{I}_i\left(y_i^n \circ [y^n_{\mathrm{mean}}]^{-1}(\mathrm{x}^h)\right), \tag{3}$$

where

– N refers to the size of the dataset,

- x^h is the original grid,
- $\mathcal{T}_i$ are the DCE-MR images ($i = 1, 2, \ldots, N$),
- y_i^n is the mapping that aligns the i^{th} image in the sequence to the n^{th} reference image,
- y_{mean}^n is the mean of the transformations y_i^n at the n^{th} iteration, and
- $y_i^n \circ [y_{\text{mean}}^n]^{-1}$ is the composition of y_i^n with the inverse of y_{mean}^n.

Performing the update process described in (3) leads to an average geometry $\mathcal{R}_{\text{mean}}$ and a collection of transformations aligning the subjects to $\mathcal{R}_{\text{mean}}$.

In our implementations, we used the following approximation for the inverse of the average transformation field y_{mean}^n:

$$\left[y_{\text{mean}}^n(\mathrm{x}^h)\right]^{-1} \approx -y_{\text{mean}}^n(\mathrm{x}^h) + 2\mathrm{x}^h. \tag{4}$$

A detailed outline of the groupwise registration framework is given in our previous work [10].

4 Experiments and Results

A sequence of abdominal MR images was used for validation. The scans were acquired with a T1-weighted FSPGR sequence. Spatial resolution was 1.88 mm by 1.88 mm by 8 mm in the S/I, L/R, and A/P directions respectively. Temporal resolution was approximately 3.7 seconds per volume [7].

We applied the proposed groupwise algorithm to visually assess how well it eliminates real and complex patient motion. For quantitative validation, the groupwise scheme was applied to a dataset with simulated motion. The resulting sequence of registered images is then compared against the ground truth (the motionless dataset). For experiments that made use of the SSDIC metric, the standard deviation was chosen heuristically to be $\sigma = 2.7$.

4.1 Real Patient Motion

Every groupwise iteration was initialized by a pairwise alignment of the subjects to the current reference geometry. In Fig. 1, we demonstrate how using different distance measures can affect the overall efficiency of the proposed method. Figures 1(f) and (i) show the optimal transformations that register Fig. 1(b) to (a) obtained using the NGF and SSDIC. Figures 1(d) and (g) show the transformed versions of the template image. Observe that the NGF and SSDIC were able to align corresponding features correctly, with only slight misregistrations near the borders from using SSDIC. We also quantified the efficiency of the distance measure by computing the difference between the transformed template and the reference image. Ideally, if registration were done properly, this difference should only exhibit the regions with contrast differences. This was the case with the NGF and the SSDIC, as demonstrated in Figs. 1(e) and (h).

Next, we present results obtained from separate experiments using two significantly different initial reference images (one before and one after the contrast

Table 1. Mean Squared Error of the SI curves as a measure of the accuracy of the registration methods.

	ROI 1				ROI 2			
α	PW-NGF	GW-NGF	PW-SSDIC	GW-SSDIC	PW-NGF	GW-NGF	PW-SSDIC	GW-SSDIC
100	1.68E-03	1.36E-04	2.01E-03	2.20E-03	4.91E-04	1.79E-04	1.61E-02	1.57E-02
200	1.20E-03	2.18E-04	6.40E-04	6.81E-04	5.34E-04	1.86E-04	4.81E-03	4.84E-03
600	2.12E-04	6.34E-05	7.10E-04	7.68E-04	3.30E-04	8.02E-05	1.10E-03	9.77E-04

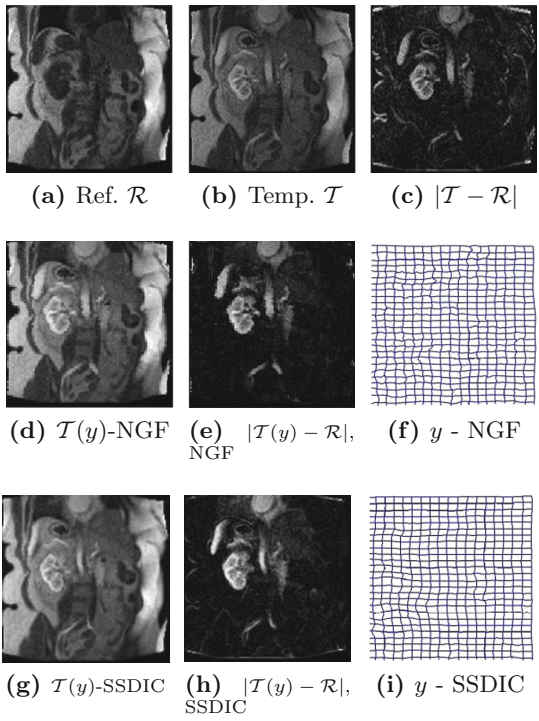

(a) Ref. $\mathcal{R}$ **(b)** Temp. $\mathcal{T}$ **(c)** $|\mathcal{T} - \mathcal{R}|$

(d) $\mathcal{T}(y)$-NGF **(e)** $|\mathcal{T}(y) - \mathcal{R}|$, NGF **(f)** y - NGF

(g) $\mathcal{T}(y)$-SSDIC **(h)** $|\mathcal{T}(y) - \mathcal{R}|$, SSDIC **(i)** y - SSDIC

Fig. 1. Results of Pairwise Registration of DCE-MR images. (a) reference, (b) template image, (c) difference image between the template and reference, (d) and (g) are the transformed templates, (e) and (h) are the difference images between the transformed template and the reference image, (f) and (i) are the optimal transformations aligning the template to the reference image using different distance measures.

agent had been absorbed) in order to demonstrate that the proposed method for correcting motion in DCE-MR datasets is indeed unbiased regardless of the chosen initial reference. Figures 2(a) and (d) show the two initial reference images used. Next to the reference images are the final mean images computed using the NGF and SSDIC, respectively. Notice that the groupwise scheme converged to the same final average image when the same distance measure was used.

Table 2. Standard Deviation of the SI curves as means of quantifying the amount of remaining motion in the sequence of registered images.

	ROI 1				ROI 2			
α	PW-NGF	GW-NGF	PW-SSDIC	GW-SSDIC	PW-NGF	GW-NGF	PW-SSDIC	GW-SSDIC
100	2.71E-02	2.48E-02	2.82E-02	2.88E-02	1.79E-02	1.43E-02	5.12E-02	5.27E-02
200	2.29E-02	2.27E-02	2.69E-02	2.95E-02	2.32E-02	2.15E-02	5.00E-02	5.03E-02
600	2.48E-02	2.43E-02	2.78E-02	2.88E-02	3.47E-02	3.46E-02	4.77E-02	4.75E-02

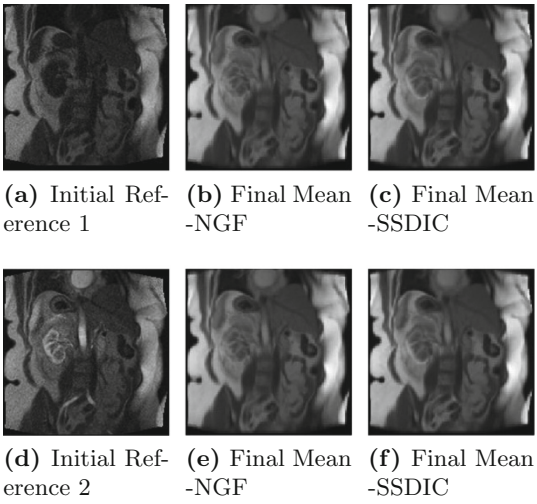

(a) Initial Reference 1 **(b)** Final Mean -NGF **(c)** Final Mean -SSDIC

(d) Initial Reference 2 **(e)** Final Mean -NGF **(f)** Final Mean -SSDIC

Fig. 2. Unbiased groupwise registration. The computation of the final mean image is independent of the initial reference.

For instance, the final mean images Fig. 2(b) and (e) are the same in spite of "evolving" from different initial references.

In Fig. 3, we show the rate of convergence of the groupwise scheme by plotting the average change in pixel values between successive iterates for the reference image against the iteration number. After around seven iterations, the average change in intensity values dropped from approximately 0.08 to 0.005, where the intensity values of the images in the dataset lie in the interval [0,1].

4.2 Simulated Motion

Simulated motion was added to a motionless dataset similar to [7]. Non-rigid diaphragm motion during respiration combined with rigid rotations at point x during time t was modelled by

$$\Delta SI(x,t) = \Delta SI_{\max} \sin\left(\frac{\pi x}{x_{\max}}\right) \left|\sin\left(\frac{\pi t}{t_b}\right)\right|.$$

In the above equation, $\Delta SI_{\max}$ is the maximum SI displacement, $x_{\max}$ is the maximum LR extent of the patient, and t_b is the duration of a full breath.

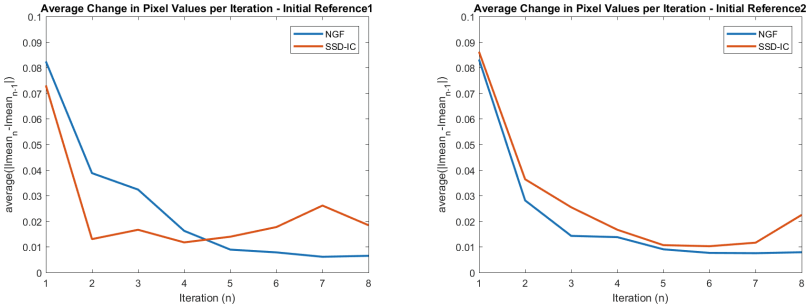

(a) Reference Image: Figure 2(a) **(b)** Reference Image: Figure 2(e)

Fig. 3. Convergence of the groupwise algorithm to a stable mean image.

Signal Intensity Curves as Measures of Accuracy. We present statistics on the signal intensity (SI) versus time curves over small regions of interest (ROIs). The ROIs considered are regions with relatively large motion shifts that are also affected by the administration of the contrast agent. They are shown in Fig. 4. SI curves give us an idea of how well the registration corrects motion in the dataset. Without motion, these curves would be smooth. However, naturally occurring motion present in our dataset introduced changes unrelated to the uptake of the contrast agent.

In Fig. 5, we display the SI curves after performing pairwise (PW) registration and groupwise (GW) registration for the NGF and SSDIC. All 4 methods were able to mitigate the effects of diaphragm motion and contrast change as demonstrated by smaller peaks in their SI curves compared to that from the simulated data. However, it is important to note the persistence of high fluctuations after using the SSDIC with either a pairwise or groupwise approach. This signifies misregistration in the specified region of interest. On the other hand, we obtained relatively smoother curves for the same ROIs after combining groupwise registration with NGF. See Figs. 5(b), (d).

We measured the mean-squared error for each curve to quantify how close our final registered images are to the ground truth. Out of all the methods we implemented, GW-NGF had the smallest mean-squared error. In some cases, it

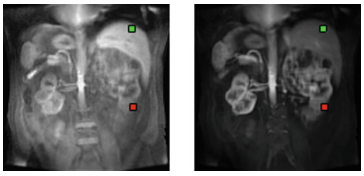

Fig. 4. Regions of interest considered in the sequence of DCE-MR data with simulated motion. Green = ROI1; Red = ROI2 (Color figure online)

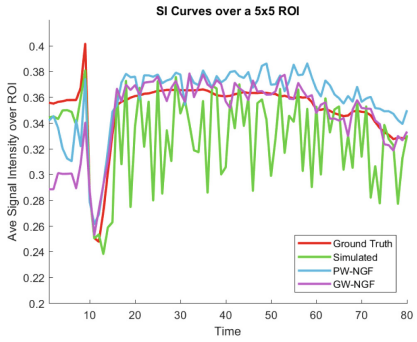

(a) PW-NGF vs GW-NGF, ROI1

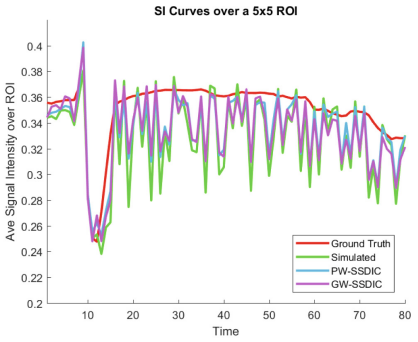

(b) PW-SSDIC vs GW-SSDIC, ROI1

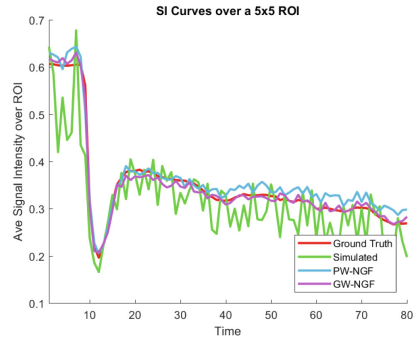

(c) PW-NGF vs GW-NGF,ROI2

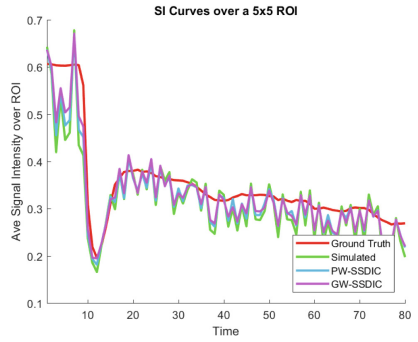

(d) PW-SSDIC vs GW-SSDIC,ROI2

Fig. 5. The signal intensity vs. time curves pre- and post-pairwise and groupwise registration for different ROIs.

even resulted to a ten-fold improvement in the MSE compared with the other methods.

The standard deviation was also calculated to quantify the amount of motion in the registered images. Again, the GW-NGF yielded the best results, implying that there were smaller fluctuations in the SI curves and less misregistrations in the ROIs considered. On the other hand, using the SSDIC with the groupwise scheme was either a hit or miss. Notice from the convergence of the method visualized in Fig. 3 that the final average change in pixel values fluctuated close to the initial average change in intensity values. This could suggest that the final reference image might be similar to the initial reference and that some of the motion correction made in the previous iterations were cancelled out.

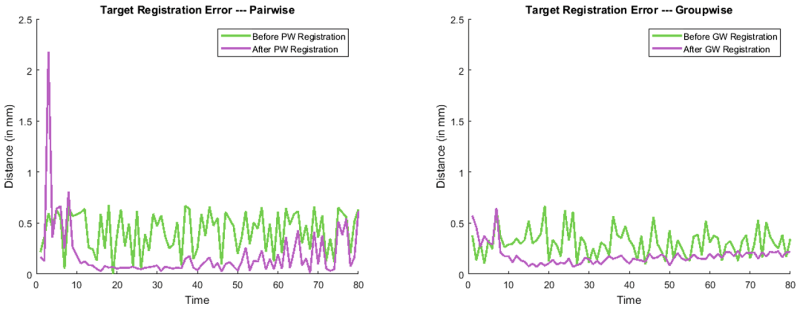

(a) TREs - Pairwise **(b)** TREs - Groupwise

Fig. 6. The location x of the center of ROI1 was tracked in the sequence of both the motion-corrupted (pre-registration) and motion-corrected images. The TREs are the distances of these centers from their correct location in the motionless dataset.

Target Registration Errors as Measures of Accuracy. Target registration errors (TRE) are defined as the distances of pixels from their initial location in the motionless dataset pre- and post-registration. Let

- ϕ_i be the transformation that warps the initial reference image to the i^{th} motion-simulated image I_i,
- y_{PW_i} the transformation that aligns the i^{th} simulated image to the initial reference,
- y_{GW_i} the transformation that aligns the i^{th} simulated image to the final reference, and
- ψ the transformation aligning the final groupwise mean to the initial reference image.

Then the pairwise TREs before and after registration, respectively, are given by

$$|x - \phi_i(x)| \text{ and } |x - \phi_i(y_{\text{PW}_i}(x))|.$$

On the other hand, the groupwise TREs are given by

$$|x - \psi(\phi_i(x))| \text{ and } |x - \psi(\phi_i(y_{\text{GW}_i}(x)))|.$$

Shown in Fig. 6 are the TREs for both PW-NGF and GW-NGF. Observe that the TRE post-GW registration had a smaller average compared to the usual pairwise approach. These are consistent with the results we obtained by analyzing the average signal intensity values over the same ROI in the previous section.

5 Conclusions

In this paper, we presented a computationally efficient and unbiased groupwise registration approach for correcting motion in a sequence of dynamic contrast-enhanced images. We also demonstrated how different distance measures affect

the performance of a multilevel elastic registration algorithm for registering contrast-enhanced images and found that both the NGF and SSDIC are able to account for contrast changes between the template and reference images. Finally, we conclude that the groupwise approach combined with the NGF yielded the smoothest SI curves and the smallest TREs, implying that this method eliminates motion more accurately than methods that simply register against an arbitrarily chosen image from the dataset.

Acknowledgments. This work was supported in part by an NSERC Discovery grant and Deborah Saucier Early Researcher Award for Mehran Ebrahimi. Mia Mojica is supported by an Ontario Trillium Scholarship (OTS). The authors would like to acknowledge Dr. Anne Martel of Sunnybrook Research Institute, Toronto, Ontario, Canada for great discussions and for providing the DCE-MRI data.

References

1. Ebrahimi, M., Lausch, A., Martel, A.L.: A Gauss-newton approach to joint image registration and intensity correction. Comput. Methods Programs Biomed. **112**(3), 398–406 (2013)
2. Ebrahimi, M., Martel, A.L.: A general PDE-framework for registration of contrast enhanced images. In: Yang, G.-Z., Hawkes, D., Rueckert, D., Noble, A., Taylor, C. (eds.) MICCAI 2009. LNCS, vol. 5761, pp. 811–819. Springer, Heidelberg (2009). https://doi.org/10.1007/978-3-642-04268-3_100
3. Geng, X., Christensen, G.E., Gu, H., Ross, T.J., Yang, Y.: Implicit reference-based group-wise image registration and its application to structural and functional MRI. Neuroimage **47**(4), 1341–1351 (2009)
4. Helm, P.A.: A novel technique for quantifying variability of cardiac anatomy: application to the dyssynchronous failing heart. Ph.D thesis, The Johns Hopkins University 164 (2005)
5. Jansen, M., Kuijf, H., Veldhuis, W., Wessels, F., Van Leeuwen, M., Pluim, J.: Evaluation of motion correction for clinical dynamic contrast enhanced MRI of the liver. Phys. Med. Biol. **62**(19), 7556 (2017)
6. Kim, M., Wu, G., Shen, D.: Groupwise registration of breast DCE-MR images for accurate tumor measurement. In: 2011 IEEE International Symposium on Biomedical Imaging: From Nano to Macro, pp. 598–601. IEEE (2011)
7. Lausch, A., Ebrahimi, M., Martel, A.: Image registration for abdominal dynamic contrast-enhanced magnetic resonance images. In: 2011 IEEE International Symposium on Biomedical Imaging: From Nano to Macro, pp. 561–565. IEEE (2011)
8. Martel, A., Froh, M., Brock, K., Plewes, D., Barber, D.: Evaluating an optical-flow-based registration algorithm for contrast-enhanced magnetic resonance imaging of the breast. Phys. Med. Biol. **52**(13), 3803 (2007)
9. Modersitzki, J.: FAIR: Flexible Algorithms for Image Registration, vol. 6. SIAM (2009)
10. Mojica, M., Pop, M., Sermesant, M., Ebrahimi, M.: Multilevel non-parametric groupwise registration in Cardiac MRI: application to explanted porcine hearts. In: Pop, M. (ed.) STACOM 2017. LNCS, vol. 10663, pp. 60–69. Springer, Cham (2018). https://doi.org/10.1007/978-3-319-75541-0_7

11. Peyrat, J.M., et al.: A computational framework for the statistical analysis of cardiac diffusion tensors: application to a small database of canine hearts. IEEE Trans. Med. imaging **26**(11), 1500–1514 (2007)
12. Sun, Y., Yan, C.H., Ong, S.-H., Tan, E.T., Wang, S.-C.: Intensity-based volumetric registration of contrast-enhanced MR breast images. In: Larsen, R., Nielsen, M., Sporring, J. (eds.) MICCAI 2006. LNCS, vol. 4190, pp. 671–678. Springer, Heidelberg (2006). https://doi.org/10.1007/11866565_82
13. Tofts, P.: T1-weighted DCE imaging concepts: Modelling, acquisition and analysis. MAGNETOM Flash **3**, 30–39 (2010)